Biomimetic Structural Electrochemistry from Conducting Polymers: Processes, Charges, and Energies. Coulovoltammetric Results from Films on Metals Revisited

Toribio F. Otero, Mercedes Alfaro, Venancio Martinez, Maria A. Perez, and Jose G. Martinez*

Oxidation/reduction reactions in films of conducting polymers exchanging anions and solvent during reactions are revisited here and explored by voltammetric and coulovoltammetric results using Pt electrodes coated with films of different polymers, in different solvents and salts. The reactions induce molecular (conformational) and macroscopic (relaxation, swelling, shrinking, and compaction) structural changes. Coulovoltammetric loops constitute a direct graphical tool to identify, separate, and quantify the structural components of the reversible film reactions together the potential domains and the charges involved in irreversible reactions. Any abrupt slope variation is related to abrupt changes of the reaction rate associated with each of the structural induced processes. Charges, energies, and characteristic potentials for any of the structural or irreversible process are obtained. Reversible film reactions are present from –1.5 to 0.35 V versus Ag/AgCl, overlapping the irreversible hydrogen evolution at the metal/polymer interface below –1.1 V. Structural reduction energies are higher than structural oxidation energies and structural changes are energetically asymmetric. 3D reactive structural memories are envisaged stepping up storage density by orders of magnitude. Conducting polymers are 3D structural gel reactors at the polymer chain level: large anions in solution cannot penetrate inside the film. Composition changes and structural processes mimic intracellular matrix (ICM) biological reactions.

1. Introduction

Electrochemical reactions in conducting polymers (CPs),[1–8] as films coating metal electrodes or as self-supported electrode films, transforms those materials (Reaction 1 for a prevalent exchange of anions between the film and the electrolyte) into the simplest biomimetic material model of the intracellular matrix (ICM) in living cells.

$$(Pol^*)_s + n\left(A^-\right)_{sol} + m(S)\left[(Pol)^{n+}\left(A^-\right)_n(S)_m\right]_{gel} + ne^- \quad (1)$$

Prof. T. F. Otero, M. Alfaro, V. Martinez, M. A. Perez, J. G. Martinez
Centre for Electrochemistry and Intelligent Materials (CEMI). Universidad Politécnica de Cartagena. Aulario II Paseo Alfonso XIII, E-30203 Cartagena (Murcia), Spain
E-mail: toribio.fotero@upct.es

DOI: 10.1002/adfm.201203502

where the oxidized material, $(Pol^{n+})(A^-)_n(S)_m$, is a dense gel constituted by partially oxidized chains (Pol^{n+}), counterions (A^-), and solvent (S); n ranging from zero to several hundreds,[9,10] and Pol^* represents the active centers on chains understood as those points where a positive charge will be stored after oxidation. Most of the reactions originating biological functions involve reactive macromolecules (biopolymers), conformational changes, ions and water exchange.

Neutral conducting polymer chains formed by heteroaromatic monomers (polypyrroles, polythiophenes, polyfuranes, etc.) have a σ bond between consecutive monomeric units allowing its rotation. Any chain surrounded by solvent molecules can move through hundreds of different conformations. After oxidation radical cations or dications are formed, giving a planar structure and hindering rotations between monomeric units. The reaction induces conformational movements of the chains giving molecular motors.[11]

When those reactions occur in films the conformational movements of the chains induce macroscopic swelling, shrinking, compaction and relaxation of the structure in order to generate or destroy the free volume required to lodge (reaction 1) charge balance counterions and solvent.[12,13] Both, molecular and macroscopic structural variations induce changes on the electrochemical responses[14–25] being theoretically described by the electrochemically stimulated conformational relaxation (ESCR) model.[26–31]

Rising packed conformational structures used as initial states to study the oxidation kinetics give reaction coefficients, activation energies and the reaction orders changing as a function of (contain information about) the initial structural state.[12] Their empirical variation is also described by the ESCR model: the chemical kinetics becomes structural chemical kinetics (SCK). Most of the biological reactions involving proteins, enzymes or nucleic acids also include conformational and folding/unfolding processes that now could be described by the SCK model.[32,33] The ESCR model physically and mathematically describes and quantifies the different structural components of the reactions.

Nevertheless quite elaborated mathematical procedures, few suitable for non-specialists, were required to separate each of those structural components. Here we will revisit voltammetric and coulovoltammetric responses from different CPs.[27,28] The final aim is getting a direct graphical methodology (that can be used by any non-specialist) to detect, identify, separate and quantify the structural components of polymeric and macromolecular reactions.

The key scientific and technological point related to CPs is that only the charge involved in their reversible oxidation/reduction is useful for the quantitative description of its reaction induced biomimetic properties and devices (artificial muscles, batteries or supercapacitors, electrochromic devices, smart membranes, smart drug delivery devices, wettability control or artificial synapses).[34,8] The optimization of either the devices actuation rates, its lifetimes and efficiencies require methodologies providing a fast and easy: a) detection of the reversible and irreversible reaction components and b) quantification of the different structural components of the reversible film reaction (potential domains, charges and energies).

1.1. Structural Electrochemistry: the ESCR Model

Structural electrochemical responses from CPs were described and quantified by the ESCR model.[9,12,15,18,26–31,35–49] Each of the constitutive polymer chains of a film can be oxidized (if they have low first, second, ..., n^{th}, ionization potentials) or reduced (for low first, second, ..., n^{th}, electronic affinities) involving the extraction or the injection, respectively, of n consecutive electrons through steps of one electron per step.[10]

The reaction goes on through n consecutive energetic conformational (electronic) states of the polymeric chain, with increasing number of conjugated planar segments. The reaction drives conformational movements of the chains giving molecular motors:[1,8,10]

$$CP + (A^-)_{sol} \leftrightarrow (CP^+)A^- + e^-$$
$$(CP^+)A^- + (A^-)_{sol} \leftrightarrow (CP^{2+})A_2^- + e^-$$
$$(CP^{2+})A_2^- + (A^-)_{sol} \leftrightarrow (CP^{3+})A_3^- + e^-$$
$$(CP^{3+})A_3^- + (A^-)_{sol} \leftrightarrow (CP^{4+})A_4^- + e^-$$
$$(CP^{4+})A_4^- + (A^-)_{sol} \leftrightarrow (CP^{5+})A_5^- + e^-$$
$$\text{---}$$
$$n)(CP^{(n-1)+})A_{n-1}^- + (A^-)_{sol} \leftrightarrow (CP^{n+})A_n^- + e^-$$

Most of the chains are located inside the film and the balancing counterion must diffuse through the film towards the chain active centre. The conformational movements must generate the required free volume to lodge counterions and solvent: the polymer film relaxes and swells during oxidation; shrinking, closing and compacting (**Figure 1**) during reduction.[50–60] So, the diffusion of the counterions across the film is the reaction rate-limiting step in swollen-open gels and conformational movements control the kinetics in shrunk and closed films.[30]

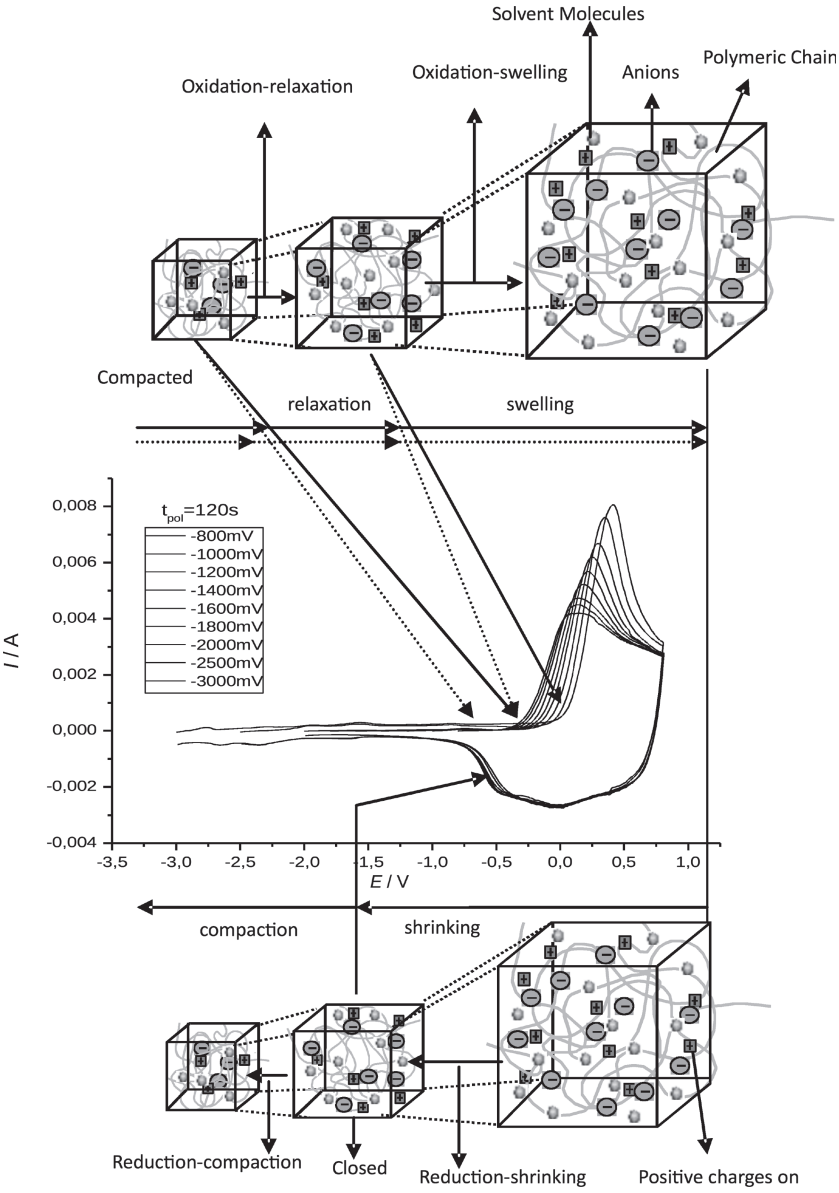

Figure 1. Voltammograms obtained from a PEDOT film in 0.1 M $LiClO_4$ acetonitrile solutions, between different cathodic potentials (–800, –1000, –1200, –1400, –1600, –1800, –2000, –2500 and –3000 mV), kept for 120 s, and the same anodic potential (800 mV) vs. Ag/AgCl, at 0.1 V s^{-1} and 25 °C showing structural relaxation/swelling and shrinking/packing processes.

2. Results

2.1. Influence of the Cathodic Potential Limit on Voltammetric and Coulovoltammetric Responses

Steady states voltammograms were attained after two consecutive potential cycles applied to a polypyrrole coated platinum

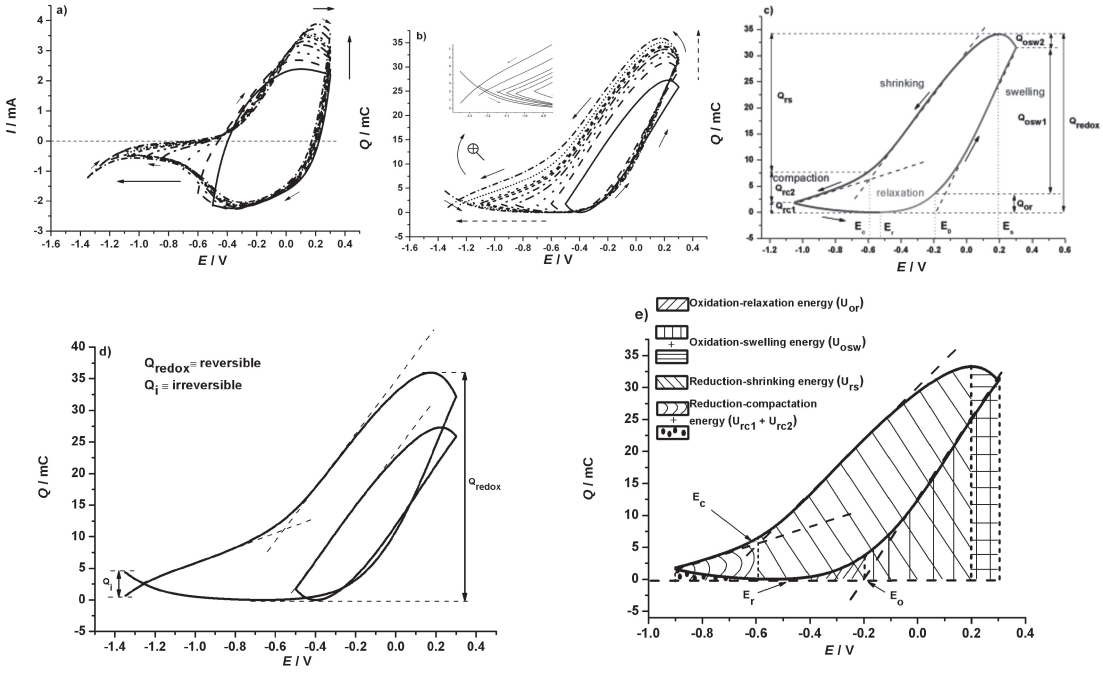

Figure 2. a) Voltammograms obtained from a polypyrrole film coating a Pt electrode in 0.1 M NaCl aqueous solution at 50 mV s^{-1} from different cathodic potential limits to 0.3 V. b) Coulovoltammograms obtained by integration of the voltammograms from (a) with expansion (inset) of the cathodic potential's region. c) Coulovoltammogram from –1.05 V to 0.3 V quantifying charges consumed by each of the structural faradic components. Q_{redox} is the redox charge; Q_{osw1} and Q_{osw2} are the oxidation-swelling charges; Q_{or} is the oxidation-relaxation charge, Q_{rs} is the reduction-shrinking charge, $Q_{rc1}$and $Q_{rc2}$are the reduction-compaction charges. E_c is the closing potential; E_r is the relaxation potential; E_o is the oxidation potential; and E_s is the swelling/shrinking transition potential. d) Closed coulovoltammogram starting from –0.5 V shows one reduction kinetic (slope Q/E). Open coulovoltammogram starting from –1.35 V shows two reduction kinetics inside the closed loop, being Q_{redox} the reduction/oxidation reversible charge, and Q_i the irreversible charge. e) Every surface area represent the energy (coulomb × volt) consumed by each of the oxidation or reduction processes.

electrode at 50 mV s^{-1}, in 0.1 M NaCl aqueous solution up to a constant anodic potential limit of 0.30 V versus Ag/AgCl (in this paper all potentials are referred to this electrode) from increasing cathodic potential limits. The memory[14,16–22] of any previous structural change was erased after the first cycle, getting steady state voltammetric responses, **Figure 2**a, on the consecutive cycles. Different facts can be underlined from the figure:

- In the cathodic branch low current flows (the reduction goes on) beyond –0.6 V.
- Reduction currents still flow at the beginning of the subsequent anodic potential sweep.
- For increasing cathodic potential limits up to –1.35 V, the oxidation maxima presents rising currents, indicating that deeper film reductions were got until that limit.
- Beyond –1.15 V the reduction current rises pointing to the presence of a new reduction process.

Several basic questions emerge about: a) the cathodic potential limit where the film reduction ends, b) the potential range for the reversible oxidation/reduction of the film, c) the nature of the new reduction process beyond –1.1 V, d) if this reaction is reversible or irreversible, and e) the way to quantitatively separate the different reversible or irreversible reactions there involved.

The key point is that only the charge involved in the reversible film reaction 1 is useful for the quantitative description of either electrochemical properties and electrochemical devices of conducting polymers.[3,8] After revision of the literature the most efficient way to separate the different components (reactions and structural processes) from the electrodic responses is coulovoltammetry.[31] By integration of the voltammetric results from Figure 2a coulovoltammetric responses (charge, Q, versus potential, E), Figure 2b are attained.

2.1.1. Redox Reversibility and Detection of Irreversible Processes

The coulovoltammetric minimum (Figure 2b) was taken as the zero charge reference: oxidation reactions give positive charge increments while reduction reactions give negative charge increments.

Closed coulovoltammetric loops were got up to a cathodic potential limit of –1.1 V. That means that inside the potential range from –1.1 to 0.30 V, the film follows reversible redox processes: the oxidation charge equals the reduction charge.

The charge difference between the loop minimum and the loop maximum is redox charge (Q_{redox}, Figure 2c) involved in reversible film reactions. Q_{redox} increases (Figure 2b) for rising cathodic potential limits.

As a partial conclusion in the potential range from –1.1 to 0.30 V only reversible film reactions occur.

Ahead –1.15 V the coulovoltammetric responses shows two well differentiated parts: a) A closed loop related to the reversible redox processes in the film, and b) an open part outside the loop (Figure 2b inset). The charge increment outside the loop is always, during the anodic or the cathodic potential sweep, negative indicating that an irreversible reduction is initiated ahead –1.1 V. The involved charge, Q_{ir}, is obtained by difference (Figure 2d) between the beginning and the end of the open coulovoltammetric part.

The charge of the closed loop (Q_{redox}) increases for rising cathodic potential limits between –1.15 and –1.5 V: the polymer reduction goes on up to the cathodic potential limit of –1.5 V overlapping, between –1.15 and –1.5 V,the above identified irreversible reaction.

2.1.2. Reversible Charge and Material Composition Shift

The magnitude of any electrochemical properties shifts, and any device works, driven by the film composition $[(Pol^{n+})(A^-)_n(S)_m]$ variation during reaction 1.[3,8] The concentration of the counterions in the film is quantified, at any point of the coulovoltammetric response, by the charge Q (mC or mA h), through the Faraday's law.

Taking into account the mass (m) of the dry reduced polypyrrole film (m = 0.180 mg), its density (ρ = 1540 g L^{-1})[61] and the charge balance (every positive charge on a chain requires the presence of a Cl^- ion), the driving charge at any point of the loop can be given as specific charge (per mass unit of reduced polymer):

$$q = Q/m(\mathrm{Cg^{-1}}) \tag{2}$$

The specific concentration of counterions $[A^-]_{ox}$ and active centres $[Pol^*]$ in the reduced film are:

$$[A^-]_{ox} = [Pol^*]_{red} = Q/[Fm](\mathrm{mol\ g^{-1}}) \tag{3}$$

where F is the Faraday constant (F = 96 485 C mol^{-1});

The volumetric concentration of counterions in the oxidized film is given by:

$$[A^-]_{ox} = [Pol^*]_{red} = [Q\rho]/[Fm](\mathrm{mol\ L^{-1}}) \tag{4}$$

The experimental determination of film volume and density variations during reaction is a difficult task. That means that specific concentrations (mol g^{-1}), defined per weight unit of a well-defined reduced state of the dry films, results more convenient for describing electrochemical properties or for the engineering design of electrochemical devices.

2.1.3. Reversible and Irreversible Reduction Charges

The overall charge involved in reduction processes (Q_{red}) during each coulovoltammetric cycle up to more cathodic potential limits than –1.15 V (Figure 2d) is:

$$Q_{red} = Q_{redox} + Q_{ir} \tag{5}$$

Coulovoltammetric responses allow a good graphical separation, identification and quantification of the charges involved in reversible, Q_{redox}, or irreversible, Q_{ir}, reduction reactions moreover they allow a good identification of the cathodic potential, –1.15 V, where irreversible reactions are initiated.

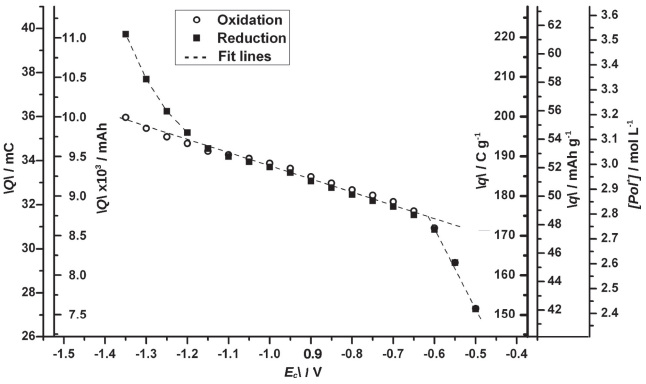

Figure 3. Total oxidation and total reduction charges [mC or mAh], specific charges [C g^{-1} or mA h g^{-1}] and concentration of active centres, $[Pol^*]$ [mol L^{-1}] obtained from the coulovoltammograms (Figure 2b) or by integration of the voltammograms (Figure 2a) through Equation 2, Equation 3 or Equation 4, for the different cathodic potential limits. The dashed lines fit experimental results.

2.1.4. Identification of Different Reversible Processes: Potential Ranges

Figure 3 presents Q_{redox}, Q_{ir} and the specific concentrations of ions and active centres in the CP film for different cathodic potential limits. Three different regions are identified:

From –0.5 to –0.6 V oxidation and reduction magnitudes (charges and film concentrations) overlap (reversible reaction) following a linear variation with the cathodic potential limit (R^2 = 0.99, where R is the correlation coefficient):

$$Q = 0.009 - 0.036\ \mathrm{V(slope - 0.036\ CV^{-1})} \tag{6}$$

From –0.65 V to –1.1V the reversibility of the film reaction goes on being the linear increase (R^2 = 0.99) of the charge with the cathodic potential limit 7 times slower (–0.005 vs. –0.036 C V^{-1}):

$$Q = 0.028 - 0.0056\ \mathrm{V(slope = -0.005\ CV^{-1})} \tag{7}$$

For more cathodic potential limits than –1.15 V the charge has two components: Q_{redox} and Q_{ir}. The linear increase (Equation 7) of the charge consumed by the reversible film oxidation/reduction (open circles, Figure 3) goes on ahead –1.15 V.

2.1.5. Deepest Attained Reduced State

The deepest reduced state attained by the material as a function of the cathodic potential limit is quantified by the highest reversible charge (Q_{redox}) of the closed loop (Figure 2d). As deduced from Figure 3 the linear increase of Q_{redox} (open circles) goes on beyond –1.35 V, without attaining any stationary state.

As a preliminary conclusion it can be stated that the film, even after attaining high reduction potential limits (from –1.15V to –1.35 V), gets a partial reduced state.

2.1.6. Structural Components of the Reversible Reduction Charge

The closed redox loop of the coulovoltammograms presents abrupt slope variations (Figure 2b–e). The slope at any point indicates the reaction rate per unit of potential variation:

$$dQ/dV = d[A^-]/dV = d[A^-]/\upsilon dt \quad (8)$$

where Q is the charge at the considered point of the coulovoltammogram, $[A^-] = Q/Fm$ is the specific concentration of counterions in the material and ν, the potential sweep rate $\nu = dV/dt$. So, any abrupt change of the Q/t slope indicates a similar abrupt variation of the reaction rate ($d[A^-]/dt$) attributed by the ESCR model to structural changes in the film.

During the cathodic potential sweep the coulovoltammogram presents a maximum (Figure 2c). From the maximum the reduction rate increases (higher slopes, dQ/dV) with the reduction overpotential. Then at –0.6 V an inflexion point exists with an abrupt transition to decreasing reduction rates for higher overpotentials. We can conclude that the pPy film reduction (reaction 1) during the cathodic potential sweep takes place through two different reaction kinetics quantified, in average, by the tangent of the concomitant coulovoltammetric domain (Figure 2c,d): from the maximum up to –0.6 V a fast reduction-shrinking occurs being the evolution of the reduction charge, Q, with the applied potential, V:

$$Q_{rs} = 0.028 - 0.040\ \text{V(slope, 0.040 CV}^{-1}) \quad (9)$$

where the sub-indexes mean: *r*, reduction and *s*, shrinking of the film according with the ESCR model. The slope indicates that the polymer reduction rate decreases in average by 40 mC per V of cathodic potential shift due to the film shrinking; and a slow (low slope of the tangent) reduction-compaction takes place at more cathodic potential limits than –0.6 V:

$$Q_{rc2} = 0.011 - 0.010\ \text{V(slope, 0.010 CV}^{-1}) \quad (10)$$

where the sub-indexes mean: *r*, reduction; *c*, compaction of the film and 2 refers to the reduction compaction process 2 according with the ESCR model. The transition intersect from 40 to 10 mC V^{-1} is the closing potential –0.6 V). As conclusion the polymer film reduction goes on ahead the closing potential.

A remarkable point is that the negative charge increment (the film reduction-compaction) goes on from –1.1 V at the beginning of the consecutive anodic potential sweep until the coulovoltammetric minimum consuming the charge Q_{rc1}. That means that the reduction overpotential is still high enough and that the film at –1.1 V, after the cathodic potential sweep, still was partially oxidized and the reduction goes on. The continuous decrease of the charge supports the faradic nature (electrochemical reduction) of Q_{rc1} and Q_{rc2} charges. The continuity of the reduction compaction process between the cathodic and the anodic potential sweep is also visualized by presenting the coulovoltammetric responses as chronocoulommetric, Q versus t, responses (**Figure 4**) by using the potential sweep rate, ν (mV s^{-1}) as the conversion factor.

As a partial conclusion a coulovoltammogram is a graphical tool showing the two structural (shrinking and compaction) processes during reduction reaction 1 (backward) in CPs, allowing its clear identification and separation. Electrochemical

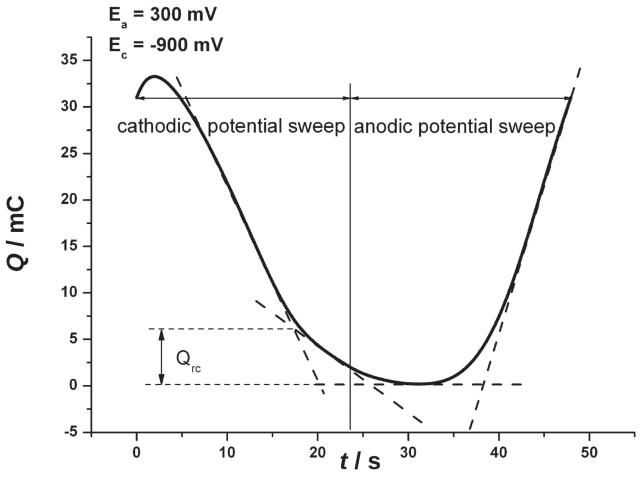

Figure 4. Chronocoulogram attained from the coulovoltammogram (–900 mV to 300 mV at 50 mV s^{-1}) using the potential sweep rate as conversion constant, showing the continuity of the faradic compaction processes (Q_{rc}) ahead the cathodic potential sweep inside the anodic potential sweep.

books and the electrochemical literature use to forget charges related to the polymer reduction-compaction considering that the polymer reduction is finished after the voltammetric reduction maximum (Figure 1 and Figure 2a) around the closing potential.

2.1.7. Structural Processes According with the ESCR Model

According with the ESCR model any CP film exchanging anions during redox reactions attains at the coulovoltammetric maximum (Figure 2c) its most oxidized and swollen gel structure: positive charges in chains, anions and solvent.[7,61–63] The fast reduction/shrinking begins from the maximum under diffusion kinetic control of the counterions across the open gel towards the solution. When the inter-chain distances equal the diameter of the counterion (probably solvated) the structure closes at –0.6 V, still under a partial oxidized state of the film. The reduction-compaction of this soft material goes on at higher overpotentials under kinetic control of the slow conformational movements of chains: the counterions must push away the chains to open its way towards the solution. The reduction rate of the film decreases at the closing potential from 0.04 (Equation 9) until 0.01 C V^{-1} (Equation 10). Structural effects explain this electrochemical paradox: higher reduction overpotentials produce during reduction/compaction slower reduction rates than those obtained at lower ovepotentials during reduction shrinking.

At the beginning of the subsequent anodic sweep the reduction overpotential and the conformational mobility still are high enough and the polymer reduction-compaction goes on until the coulovoltammetric minimum. There the oxidation is initiated by electrochemical stimulation of the conformational relaxation (oxidation/relaxation) opening the compacted structure and generating the required free volume to lodge balancing counterions arriving from the solution.[27–30] Once relaxed the

oxidation/swelling goes on under diffusion kinetic control of the counterions from the solution through the swelling film.[27–30] At the anodic potential limit the maximum anodic overpotential is attained but the counterions did not have time enough to attain every available active center of the chains inside the film: its oxidation is completed during the beginning of the cathodic potential sweep until the coulovoltammetric maximum.

In conclusion, structural changes (conformational movements of the chains, relaxation, swelling, shrinking and compaction) are driven by oxidation and reduction reactions. Coulovoltammograms present a clear graphical tool for the separation of the different structural processes mathematically defined by the ESCR model.

2.1.8. Structural Faradic Processes, Related Charges and Characteristic Potentials

Once identified the different structural domains, Figure 2c also allows a quantitative determination of the charge consumed by each of the constitutive structural faradic processes of reaction 1.

1. Reduction/compaction 1: Starting from the cathodic potential limit the slow reduction-compaction goes on until the minimum consuming the reduction/compaction charge 1 (Q_{rc1}).
2. Oxidation/relaxation: At the minimum the polymer oxidation is initiated under conformational relaxation kinetic control, consuming the oxidation/relaxation charge (Q_{or}). The strong influence of rising compaction states is clearly visualized by the oxidation-relaxation potential shift in voltammetric results (Figure 1).
3. Oxidation/swelling 1: Once relaxed the film oxidation/swelling goes on (Figure 2c) until the anodic potential limit consuming the charge Q_{osw1}.
4. Oxidation/swelling 2: The oxidation/swelling goes on at the beginning of the cathodic potential sweep (the oxidation overpotential is still high and the oxidation time was not enough during the anodic potential sweep to attain a full film oxidation) up to the maximum, consuming the charge Q_{osw2}.
5. Reduction/shrinking: After the maximum, a fast film reduction/shrinking starts consuming the reduction/shrinking charge Q_{rs}.
6. Reduction/compaction 2: After the closing potential the reduction goes on until the cathodic potential limit under slow conformational relaxation kinetic control promoting the progressive compaction of the film and consuming the charge Q_{rc2}.

Therefore, oxidation and reduction reversible charges involved in the closed loop, $Q_{redox} = Q_{ox} = Q_{red}$, can be reconstructed (Figure 2c) by addition of the different structural faradic components:

$$Q_{ox} = Q_{or} + Q_{osw} + Q_{osw2} \quad (11)$$

$$Q_{red} = Q_{rs} + Q_{rc1} + Q_{rc2} \quad (12)$$

Charges Q_{rc1} and Q_{osw2}, and the related processes illustrate the chemical inertia induced by molecular and macroscopic structural movements. The reduction/compaction process (Figure 2c) consumes over 15% of the redox charge.

The different structural regions are separated by characteristic potentials. The closing potential, E_c, separates reduction/shrinking from reduction/compaction processes. The relaxation potential, E_r, separates reduction/compaction from oxidation/relaxation processes; and the oxidation potential, E_o, separates oxidation/relaxation from oxidation/swelling processes. At the coulovoltammetric maximum, E_s, oxidation/swelling moves to reduction/shrinking processes. Figure S1 (Supporting Information) corroborates the strong influence of the cathodic potential limit on the relaxation potential, E_r, detected and described in the literature from voltammetric (Figure 1) and chronoamperometric results.[26–30] Rising reduced and compacted structures attained at higher cathodic potential limits require more energy (higher anodic overpotentials) to relax the structure.

Ignoring compaction-relaxation and irreversible reduction charges can be the origin of the accepted redox irreversibility of conducting polymers.[64–69]

2.1.9. Structural Reactive Energies. Energy Asymmetry

Energies (U, W h Kg^{-1}) consumed by each of the identified structural processes were obtained by integration of the correlated coulovoltammetric areas: $U = \int V dQ$. Figure 2e shows the areas related to each of the structural energetic components: U_{or} is the energy consumed during the film oxidation/relaxation; U_{osw} is the energy consumed during the film oxidation/swelling; U_{rs} is the energy consumed during the film reduction/shrinking, U_{rc1} is the energy consumed during the film reduction/compaction at the beginning of the anodic potential sweep; and U_{rc2} is the energy consumed during the film reduction compaction at the end of the cathodic potential sweep. Oxidation energies are positive and reduction energies are negative. The difference between oxidation and reduction energies for different cathodic (or anodic, see next point) potential limits are depicted by **Figure 5** as specific energies, u (per mass unit of reduced polymer).

The energy involved during the film oxidation is:

$$u_{ox} = u_{or} + u_{od} \quad (13)$$

The energy involved in the film reduction processes is:

$$u_{red} = u_{rs} + u_{rc1} + u_{rc2} \quad (14)$$

The most remarkable point is that the reduction energy is almost two times higher than the concomitant oxidation energy. Oxidation and reduction processes are very asymmetric from the point of view of the involved energies. This large irreversibility could indicate that those materials remember its pristine conformational structure: they were electrogenerated at anodic overpotentials as oxidized materials.[70] Moving the material away from this state by electrochemical reduction requires much more energy than that required to recover the pristine conformational state by electrochemical oxidation. The conformational structure remembers its birth state, as shape memory metals or shape memory polymers do. Deformations are produced mechanically in shape memory materials and the original shape is recovered by thermal energy. In conducting polymers deformations (shrinking) from the pristine oxidized and swollen structure are produced by supplying electrochemical energy to reduce the material; the original swollen structure being

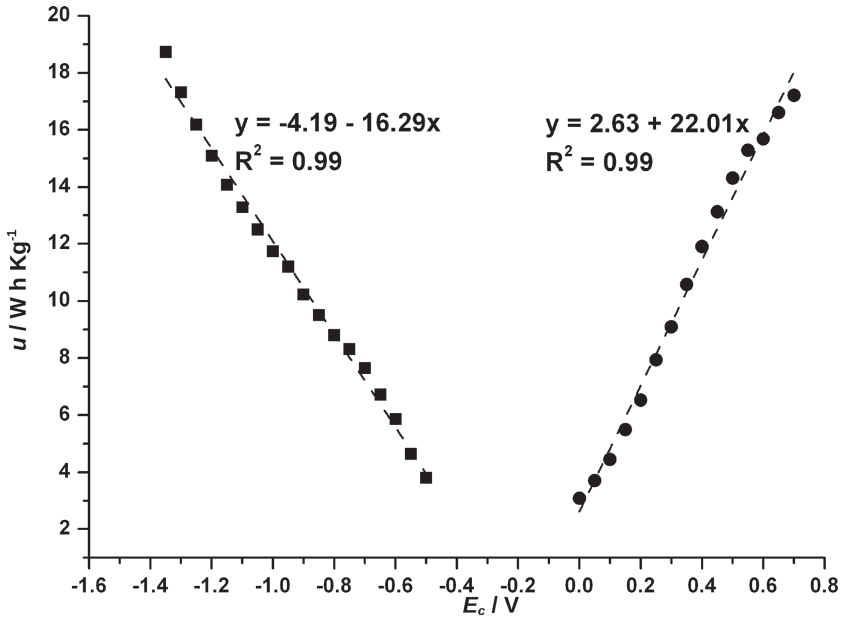

Figure 5. Evolution of the specific energy increment, $u_{red} - u_{ox}$ (W h Kg^{-1}), as a function of the cathodic or anodic potential limits for the voltammograms.

recovered by consuming a lower specific energy during electrochemical oxidation: $u_{red} >> u_{ox}$. The energy increment, $u_{red} - u_{ox}$, is shown in Figure S2 (Supporting Information) as a function of the cathodic potential limits.

A remarkable result is that most of the energy is consumed by the reduction/shrinking process (Supporting Information Figure S2, up triangles). Specific energies from Figure S2 fit linear or exponential evolution with the cathodic potential limits (see Table S1, Supporting Information).

2.2. Influence of the Anodic Potential Limit

Reversible structural reactions giving closed charge loops were obtained in Figure 2b for a range of cathodic potential limits between –0.5 and –1.1 V. Now an intermediate potential of –0.9 V was chosen as the cathodic potential limit to explore the influence of the anodic potential limit on reversible and irreversible processes, consumed charges and energies. **Figure 6**a depicts the stationary

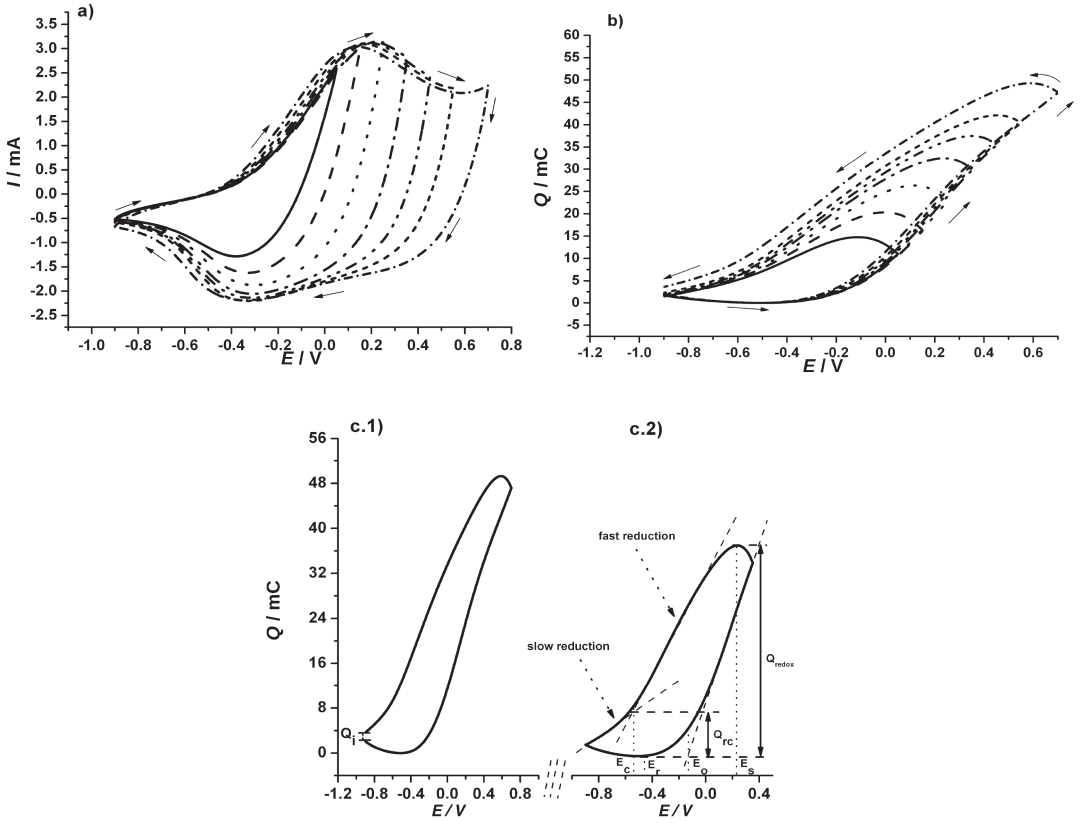

Figure 6. a) Voltammograms obtained from Pt coated polypyrrole electrode in a 0.1 M NaCl aqueous solution at a scan rate of 50 mVs^{-1} from –0.9 V until different anodic potential limits; b) Coulovoltammograms obtained by integration of the voltammograms from (a); c.1) Open loop curve shows the charge involved in the new irreversible oxidation process (Q_i) plus the redox charge; c.2) closed loop shows the reduction-compaction charge Q_{rc}, and the reversible redox film charge, Q_{redox}, the closing potential, E_c; the relaxation potential, E_n; and the oxidation potential, E_0.

voltammograms attained after three consecutive potential sweeps for each of the studied anodic potential limits.

By integration of those voltammetric results, the coulovoltammetric responses (Figure 6b) were obtained. Anodic potential limits lower than 0.35 V give closed coulovoltammetric loops: only the reversible reaction 1 occurs in the film. For more anodic potential limits than 0.35 V the oxidation charges overcome the reduction charges (Figure 6b) giving open coulovoltammetric loops: a new irreversible oxidation occurs. The charge consumed by this irreversible oxidation (Q_{iox}) is obtained by difference between charges at the beginning and at the end of the open loop (Figure 6c.1). The reversible (redox) charge is attained by deducting Q_{iox} from the coulovoltammetric charge range, Q (maximum minus minimum): $Q_{redox} = Q - Q_{iox}$.

For the studied potential limits the coulovoltammograms present the same four structural processes above described: reduction/diffusion, reduction/compaction, oxidation/relaxation and oxidation/diffusion (Figure 6c.2).

Charges and energies involved in every structural electrochemical process are presented as a function of the anodic potential limit by Figure S3 and Tables S2 and S3 in the Supporting Information. Again the large asymmetry exists between oxidation and reduction energies indicate that the materials remember its pristine structure after electrogeneration.

2.3. Irreversible Reactions Detection and Identification

The evolutions of the charges involved in irreversible oxidation (Q_{iox}) and reduction (Q_{ir}) reactions were depicted in **Figure 7**, black circles (plot b). In both cases the irreversible charge increases with the overpotential, cathodic or anodic, beyond –1.1 V or 0.35 V, respectively.

In order to clarify if the above detected irreversible electrochemical reactions are supported by the conducting polymer film or by the back metal, a clean Pt electrode was submitted to consecutive potential cycles between –1.5 and 0.9 V in 0.1 M NaCl aqueous solution at 50 mVs^{-1} (Figure 7, plot a). In parallel another Pt electrode coated with a polypyrrole film was submitted to an oxidation-degradation voltammogram[71–78] between –0.9 V and 2.2 V in 0.1 M NaCl aqueous solution at 50 mV s^{-1}(Figure 7, plot c). The anodic maximum at 1.7 V has been attributed to the polypyrrole degradation by overoxidation.[74,77,79–87]

The voltammogram from Figure 2a obtained between –1.1 V and 0.3 V also was overlapped in Figure 7 (plot d).

The evolution of the irreversible oxidation charge above 0.35 V (plot b) looks extrapolated from the degradation (overoxidation) voltammetric maximum (Figure 7, plot c) indicating that the anodic irreversible process above 0.35 V can be attributed to the beginning of the polymer degradation by overoxidation.

The hydrogen evolution on the clean Pt electrode occurs at more cathodic potentials than –1.0 V.[49] The irreversible reduction on the polypyrrole coated electrode takes place (Figure 7, plot b) above –1.1 V and can be attributed to the hydrogen release at the platinum/polypyrrole interface after water diffusion across the film. The irreversible reaction should disappear by using freestanding polymeric electrodes, eliminating the back metal. This aspect will be checked in a next paper.

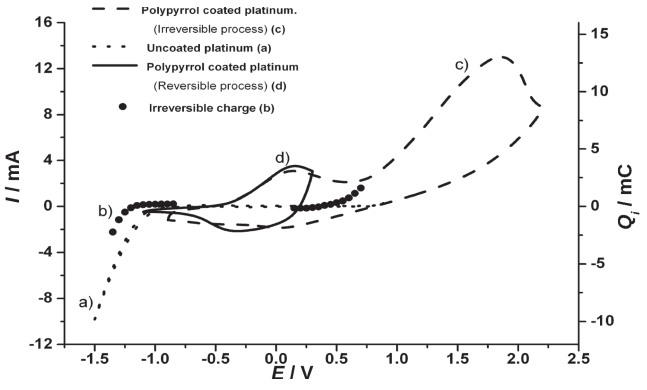

Figure 7. a) Voltammogram obtained using a clean platinum electrode between –1.5 V and 0.9 V. b) Irreversible charges consumed by irreversible anodic (Supporting Information Figure S2) and cathodic (Figure 3) processes. c) Voltammogram obtained from a polypyrrole coated platinum electrode between –0.9 V to 2.2 V. d) Voltammogram obtained from a polypyrrole film between –1.1 V and 0.3 V. Voltammograms were performed in 0.1 M NaCl aqueous solution at 50 mVs^{-1}. The films were generated at 0.85 V in 0.1 M pyrrole, 0.1 M $LiClO_4$ acetonitrile solution by consumption of a constant charge of 400 mC.

2.4. Structural Kinetic Components from Different Polymers, Electrolytes or Solvents

Figure 8 shows the attained coulovoltammograms in aqueous solutions of different salts: $LiCF_3SO_3$, $LiBF_4$or $LiClO_4$; for different solvents: water, acetonitrile or propylene carbonate, or from different conducting polymers: polypyrrole, PEDOT or poly(3-dodecylthiophene). Under those experimental conditions all those polymers exchange anions with the electrolyte during its oxidation/reduction following reaction 1.

Similar experimental coulovoltammetric responses to those described in Figure 2c with the same four structural kinetic processes were obtained from each of the studied systems.

2.5. Reactions Require Simultaneous Charge Transfer from Chains and Ion Transfer from Solution

Reaction 1 induces structural changes that (reduction-compaction and oxidation-relaxation) control the reaction rate of relaxation and compaction processes. Under those conditions it is expected that the oxidation-relaxation only will be possible when both events electron extraction from the chain and counterion arrival from the solution through the film occur simultaneously. If the anions present in the electrolyte are too big the conformational relaxation cannot produce the free volume required to the entrance of the anions from the solution. In that case the film oxidation, even for high anodic overpotentials, should not occur.

Two polypyrrole films were electrogenerated in presence of different salts. From pyrrole-NaDBS aqueous solution the electrogenerated polypyrrole film traps the DBS^- ions during

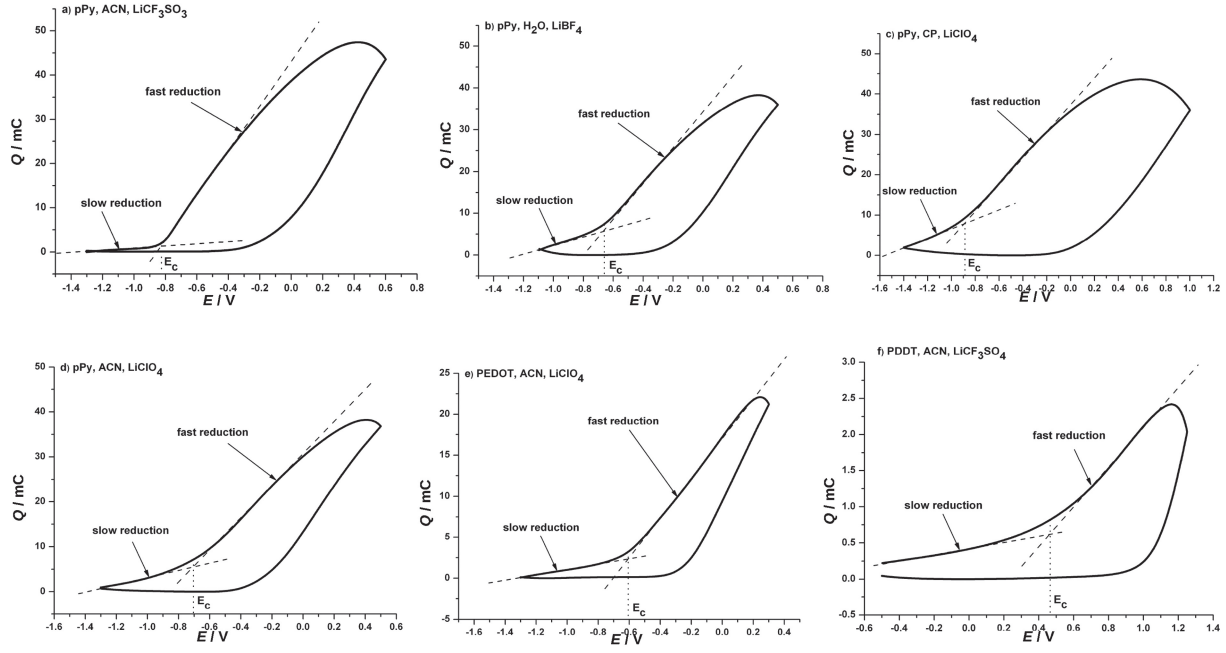

Figure 8. Coulovoltammograms obtained at 50 mV s^{-1} from different salts, solvents and polymers: a) polypyrrole film in 0.1 M $LiCF_3SO_3$ acetonitrile solution; b) polypyrrole film in 0.1 M $LiBF_4$ aqueous solution; c) polypyrrole film in 0.1 M $LiClO_4$ propylene carbonate solution; d) polypyrrole film in a 0.1 M $LiClO_4$ acetonitrile solution; e) PEDOT film in 0.1 M $LiClO_4$ acetonitrile solution; and f) PDDT film in a 0.1 M $LiCF_3SO_3$ acetonitrile solution.

growth, forcing the exchange of cations with the solution during any electrochemical control.[1,48] By using pyrrole-$LiClO_4$ aqueous solutions the generated film exchanges anions during electrochemical control.[1]

Voltammograms (**Figure 9**a) and coulovoltammograms (Figure 9b) performed from each of those films coating the Pt electrode in $LiClO_4$ solution show well defined oxidation and reduction peaks (full lines). Small ClO_4^- anion and small Li^+ cation are easily exchanged with the films. The pPy/DBS film also shows well-defined oxidation and reduction maxima when checked in 0.1 M NaPSS or NaDBS aqueous solution (Figure 9, dotted and dashed black lines). The small Na^+ is exchanged by the film.

When the polypyrrole/ClO_4^- film was checked in 0.1 M NaDBS, or in 0.1 M NaPSS aqueous solution the redox process doesn't appear (dotted and dashed red lines). The large DBS^- or PSS^{n-} anions cannot penetrate into the film even at high anodic overpotentials.

The experimental solutions have similar conductivities: 8.71, 6.24 and 4.94 mS cm^{-1} for $LiClO_4$, NaDBS and NaPSS, respectively, aqueous solution. The large oxidation/reduction charge of the pPy/ClO_4^- material in presence of ClO_4^- (>25 mC, Figure 9b) becomes very low (1.3 mC, Figure 9b inset) in presence of a large anion (DBS^- or PSS^-). Those results corroborate that the charge transfer occurs from, or to, each of the polymeric chains inside the film. If the charge transfer should occur

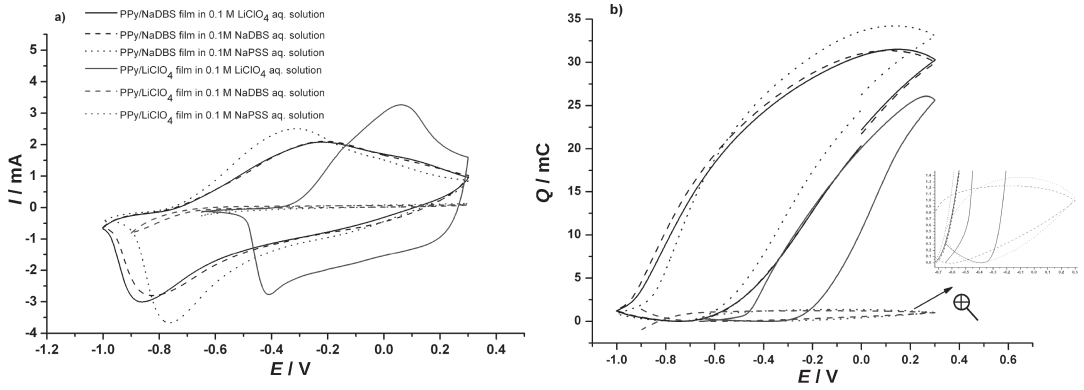

Figure 9. a) Stationary voltammograms obtained by potential cycling using polypyrrole films coating Pt electrodes, electrogenerated from 0.1 M pyrrole and 0.1 M $LiClO_4$ acetonitrile solution (red lines) or from 0.1 M pyrrole and 0.1 M NaDBS aqueous solution (black lines) and checked in: 0.1 M $LiClO_4$ aqueous solution (full lines), in 0.1 M NaDBS aqueous solution (pH = 5.46) (dashed lines) or in 0.1 M NaPSS aqueous solution (pH = 8.45) (dotted lines). b) Coulovoltammograms from Figure 10a. Scan rate of 50 mVs^{-1}.

only at the polymer/solution interface or at the porous walls the polypyrrole film generated in $LiClO_4$ should be electroactive in both, NaDBS or NaPSS but the reaction does not occur despite the high solution conductivity, high electrolyte concentration and high oxidation overpotentials.

Those results illustrate how conformational movements can induce spatial control and spatial limitations allowing, or not, the reaction to occur.

The oxidation/reduction of conducting polymers requires four conditions to occur: presence of balancing ions in the electrolyte, high conductivity of the electrolyte, overpotentials and suitable dimensions of the balancing counterions to penetrate into the film across the free volume generated by oxidation-relaxation of the polymeric chains.

As conclusion films of conducting polymers are three-dimensional molecular electrodes at the polymer chain level: they are dense reactive polymer gel electrodes (Figure 1). In a relaxed and partially oxidized structure the electrochemical interface is constituted by each of the film polymeric chains. Most of the reaction takes place inside the material along each of the constitutive chains.

2.6 Conformational Biomimetic Memory

Structural coulovoltammetric loops as those represented by Figure 2, 6b,c, 8 and 9b are similar to magnetic, mechanical or dielectric relaxation loops. These relaxation loops present an almost rhombic shape while Figure 2c presents a most rich shape including four different structural processes. In today technologies most of the information is stored in magnetic memories based on the magnetic relaxation loop that provides, for the same temperature, two stable magnetized states related to the two basic bit units (0 and 1). Shape memory alloys are being investigated to provide higher possibilities than binary storage. Figures 2b and Figure 6b show that a high number of different and reproducible energetic structural states can be stored and read by cyclic voltammetry as a function of the anodic or cathodic potential limits. Those states correspond to linear evolutions of the involved energy, Figure 5. In a similar way the SCK reveals that the stored conformational energy is a linear function of the compacted structure attained by the film reduction-compaction at rising cathodic overpotentials.[12]

All those results indicate that the number of different and reproducible memory states available to store information in three-dimensional packed reactive conformations can step up for several orders of magnitude related to today magnetic memories. A new way is open for the exploration of new three dimensional conformational, reactive and soft (wet or dry) memory devices and as a new hypothesis to investigate if our brain memory, or a fraction of it, is stored by energetic conformational states of the biopolymers inside neurones or taking place of the ionic neuron channels.

3. Conclusions

Conducting polymers are 3D electrodes (dense polymer gels) at the polymer chain level: the oxidation charge transfer only occurs when the diameter of balancing counterions is low enough to allow its penetration from the solution, through the swelling film, until every chain. The electrochemical reaction drives structural molecular (conformational) and macroscopic (relaxation, swelling, shrinking, closing and compaction) processes.

Coulovoltammograms are excellent tools for the identification of the potential ranges where reversible and irreversible reactions occur, for the separation and quantification (by charge and by energy) of the different structural processes taking place during electrochemical reactions in the film and for the quantification of the charges required by each of the structural processes. Reversible reactions give closed coulovoltammetric loops.

The presence of irreversible reduction reactions at high reduction overpotentials gives a charge loop with crossing branches that originate an open coulovoltammetric part outside the loop. The charge inside the closed loop corresponds to the charge involved, inside the studied potential range, in reversible film reactions. The charge difference between the beginning and the end of the open part gives the charge consumed by irreversible reduction reactions.

The presence of irreversible oxidation reactions at high oxidation overpotentials also gives open coulovoltammograms: the oxidation charge overcomes the reduction charge. The charge difference between the beginning and the end of the open coulovoltammogram is consumed by irreversible oxidation reactions. The charge consumed inside the studied potential range by reversible reactions in the film is got by subtracting from the full coulovoltammetric charge the charge consumed by irreversible reactions. Polypyrrole reversible oxidation/reduction (oxidation charges equal reduction charges) occurs in the full studied potential range from –1.35 V to 0.35 V. At more cathodic potentials than –1.1 V the reversible polymer reduction coexists with irreversible reactions, probably the hydrogen evolution at the polymer/metal interface. At more anodic potentials than 0.35 V a new irreversible reaction starts: the polymer degradation by irreversible overoxidation.

Inside the potential range of reversible processes only one oxidation and one reduction reaction (reaction 1) occurs through four different structural kinetic processes: oxidation-relaxation, oxidation-diffusion, reduction shrinking and reduction-compaction. Slope (dQ/dE) variations on the coulovoltammogram identify each of those structural processes.

The film reduction rate decreases when the film reduction compaction increases at rising cathodic overpotentials. The total reduction of films of conducting polymers exchanging anions, with elimination of the counterions from the film, will require very long (days or weeks) reduction times at high reduction overpotentials. The reduction time is expected to decrease with the film thickness, with the anion radius and in solvents having a high solvent-reduced polymer interaction (high solvent content in the reduced film giving a most open structure). A high fraction of the reversible reduction charge is consumed at cathodic overpotentials beyond the closing potential. At the closing potential the film keeps a high oxidation degree (a high counterion's content).

Structural and reversible oxidation and reduction processes are present in different solvents, with different salts and for

different conducting polymers having prevalent exchange of anions during reaction. Inside the reversible potential range energies involved in the reduction processes are much higher than those related to the oxidation processes. This energetic asymmetry indicates that the electrogenerated materials remember its pristine structure: they are generated in an oxidized state. Conducting polymers can store thousands of reproducible conformational energetic states. New three dimensional conformational, reactive and soft memory devices are envisaged rising the storage density by several orders of magnitude related to today magnetic memories.

4. Experimental Section

Pyrrole (Fluka 97%) and 3, 4-ethylenedioxythiophene EDOT, (Aldrich) were purified by distillation under vacuum using a diaphragm vacuum pump MZ 2C SCHOTT. Dodecylthiophene DDT (Aldrich 97%); lithium perchlorate $LiClO_4$ (Aldrich); sodium chloride NaCl (Panreac); lithium tetrafluoroborate $LiBF_4$ (Aldrich 98%); lithium trifluoromethane-sulfonate $LiCF_3SO_3$ (Aldrich 96%); acetonitrile (Panreac 99.9%); propylene carbonate (Sigma-Aldrich 99.7%); poly(sodium 4-styrene-sulfonate) Na-PSS (molecular weight 1 000 000, Aldrich); dodecylbenzenesulfonic acid, sodium salt (DBS, Aldrich); and dodecylbenzenesulfonic acid (DBSA) solution (70 wt% in 2-propanol; Aldrich) were used as received. Ultrapure water was obtained from Millipore Milli-Q equipment.

All the electrochemical studies were performed using an Autolab electrochemical workstation (PGSTAT-100 potentiostat-galvanostat) controlled using a personal computer with GPES electrochemical software. The solid-state conductivity measurements were performed using an Agilent 6 ½ digit multimeter, having a precision of 0.1 mΩ. The conductivity of the solutions was measured using a Crison conductivity meter.

A platinum electrode with a surface area of 1 cm^2 (0.5 cm^2 by side) was used as the working electrode (WE). Two clean stainless steel plates with 4 cm^2 of surface area, one by side of the WE, were used as the counterelectrodes. The reference electrode was a Crison Ag/AgCl (3 M KCl) electrode. All potentials reported in this work were referenced to this electrode. Before every electrochemical experiment the solution was deaerated by nitrogen bubbling for 10 min. After that, the nitrogen atmosphere was maintained by nitrogen flow over the solution. All the experiments were performed at 25 °C (room temperature).

Polypyrrole films were electrogenerated on a Pt electrode from a fresh 0.1 M pyrrole and 0.1 M $LiClO_4$ acetonitrile solution by potentiostatic polarization at 0.850 V. The process was stopped after consumption of 400 mC of polymerization charge.

The coated electrode was then rinsed and translated into 0.1 M NaCl aqueous solution. There it was controlled by consecutive potential sweeps from –0.65 to 0.3 V at 50 mV s^{-1} until getting a stationary voltammetric response, usually after two cycles. Through the voltammetric charge involved in reaction 1, the reproducibility of the electrogeneration processes was checked. After stopping the potential sweep at –0.65 V, the reduced electrode was rinsed, dried and weighed using a Sartorious SC2 balance with a precision of 10^{-7} g. The mass of the reduced films used in this paper was 0.180 ± 0.001 mg, obtained comparing the uncoated and the coated electrodes masses. Every coated electrode is then ready for the voltammetric studies.

Poly(3,4-ethylenedioxythiophene) (PEDOT) films were electrogenerated from 0.1 M $LiClO_4$ and 0.01 M EDOT acetonitrile solution applying a constant current (2 mA) through the working platinum electrode, consuming a total charge of 300 mC. After polymerization the coated electrode was rinsed with acetonitrile and dried before use. The mass of the reduced and dried film was 0.360 ± 0.001 mg.

Polypyrrole-DBS films were electrogenerated in 0.1 M DBS and 0.1 M pyrrole aqueous solution, keeping a constant potential of 0.7 V versus Ag/AgCl until a total charge of 400 mC was consumed (mass = 0.286 ± 0.001 mg).

Poly(3-dodecylthiophene), (PDDT) films were electrogenerated from 0.1 M $LiCF_3SO_3$ and 0.1 M 3-dodecylthiophene acetonitrile solution by flow of a constant current of 0.5 mA through the working platinum electrode until consumption of 60 mC. After polymerization the coated electrode was rinsed with acetonitrile and dried before use. The mass of the dried film was 0.050 mg.

Supporting Information

Supporting Information is available from the Wiley Online Library or from the author.

Acknowledgements

The authors acknowledge financial support from the Spanish Government (MCINN) Projects MAT2008-06702 and CTQ2007-60459 and Fundación Séneca Project 08684/PI/08, J.G.M. acknowledges the Spanish Education Ministry for a FPU grant (AP2010-3460).

Received: November 27, 2012
Revised: January 15, 2013
Published online: March 8, 2013

[1] L. V. Conzuelo, J. Arias-Pardilla, J. V. Cauich-Rodríguez, M. A. Smit, T. F. Otero, *Sensors* **2010**, *10*, 2638.
[2] T. F. Otero, *J. Mater. Chem.* **2009**, *19*, 681.
[3] T. F. Otero, J. G. Martinez, J. Arias-Pardilla, *Electrochim. Acta* **2012**, *84*, 112.
[4] H. Shirakawa, E. J. Louis, A. G. MacDiarmid, C. K. Chiang, A. J. Heeger, *J. Chem. Soc., Chem. Commun.* **1977**, 578.
[5] A. Diaz, *Chem. Scripta* **1980**, *17*, 145.
[6] A. F. Diaz, M. Salmon, *ACS Division of Petroleum Chem. Preprints* **1981**; Vol. *26*, p. 758.
[7] E. M. Genies, G. Bidan, A. F. Diaz, *J. Electroanal. Chem.* **1983**, *149*, 101.
[8] T. F. Otero, J. G. Martinez, *J. Mater. Chem. B* **2013**, *1*, 26
[9] T. F. Otero, I. Boyano, *ChemPhysChem* **2003**, *4*, 868.
[10] T. F. Otero, J. J. Sanchez, J. G. Martinez, *J. Phys. Chem. B* **2012**, *116*, 5279.
[11] T. F. Otero, in *From Non-Covalent Assemblies to Molecular Machines*, (Ed: J.-P. Sauvage, P. Gaspard), Wiley-VCH Verlag GmbH & Co. KGaA, Weinheim **2010**; pp. 443–452.
[12] T. F. Otero, J. G. Martinez, *Adv. Funct. Mater.* **2013**, *23*, 404.
[13] E. Volpi, M. Trueba, S. P. Trasatti, *Prog. Org. Coat.* **2012**, *74*, 376.
[14] K. Aoki, *J. Electroanal. Chem.* **1991**, *310*, 1.
[15] K. Aoki, M. Kawase, *J. Electroanal. Chem.* **1994**, *377*, 125.
[16] J. Heinze, B. A. Frontana-Uribe, S. Ludwigs, *Chem. Rev.* **2010**, *110*, 4724.
[17] M. Kalaji, L. M. Peter, L. M. Abrantes, J. C. Mesquita, *J. Electroanal. Chem.* **1989**, *274*, 289.
[18] G. Inzelt, *Electrochim. Acta* **1989**, *34*, 83.
[19] C. Odin, M. Nechtschein, *Phys. Rev. Lett.* **1991**, *67*, 1114.
[20] C. Odin, M. Nechtschein, P. Hapiot, *Synth. Met.* **1992**, *47*, 329.
[21] B. Villeret, M. Nechtschein, *Phys. Rev. Lett.* **1989**, *63*, 1285.
[22] M. A. Vorotyntsev, E. Vieil, J. Heinze, *J. Electroanal. Chem.* **1998**, *450*, 121.
[23] *Modern Aspects of Electrochemistry, vol. 33*, (Ed: R. E. White, J. O. Bockris, B. E. Conway) Kluwer Academic Publishers, New York **1999**.

[24] G. Inzelt, in *Monographs in Electrochemistry*; 2nd ed., (Ed: F. Scholz), Springer, Berlin, **2012**.
[25] *Electropolymerization: Concepts, Materials and Applications*, (Ed: S. Cosnier, A. Karyakin) Wiley-VCH Verlag GmbH & Co. KGaA, Weinheim **2010**.
[26] T. F. Otero, H. Grande, J. Rodríguez, *J. Electroanal. Chem.* **1995**, *394*, 211.
[27] T. F. Otero, H. Grande, J. Rodrîguez, *Electrochim. Acta* **1996**, *41*, 1863.
[28] T. F. Otero, H. Grande, J. Rodriguez, *Synth. Met.* **1996**, *76*, 293.
[29] T. F. Otero, H.-J. Grande, J. Rodríguez, *J. Phys. Chem. B* **1997**, *101*, 3688.
[30] T. F. Otero, H. Grande, J. Rodríguez, *J. Phys. Chem. B* **1997**, *101*, 8525.
[31] H. Grande, T. F. Otero, *J. Phys. Chem. B* **1998**, *102*, 7535.
[32] *Nat. Struct. Mol. Biol.* **2009**, *16*, 573.
[33] J. Buchner, L. Moroder, *Oxidative Folding of Peptides and Proteins*, RSC Publishing, Cambridge **2009**.
[34] M. Aldissi, *Intrinsically Conducting Polymers: An Emerging Technology*, Springer, Burlington, VT **1993**.
[35] H. Grande, T. F. Otero, I. Cantero, *J. Non-Cryst. Solids* **1998**, *619*, 235.
[36] H. Grande, T. F. Otero, *Electrochim. Acta* **1999**, *44*, 1893.
[37] T. F. Otero, M. Bengoechea, *Langmuir* **1999**, *15*, 1323.
[38] T. F. Otero, I. Boyano, *J. Phys. Chem. B* **2003**, *107*, 4269.
[39] T. F. Otero, I. Boyano, *J. Phys. Chem. B* **2003**, *107*, 6730.
[40] T. F. Otero, M. T. Cortes, I. Boyano, *J. Electroanal. Chem.* **2004**, *562*, 161.
[41] T. F. Otero, I. Boyano, M. T. Cortés, G. Vázquez, *Electrochim. Acta* **2004**, *49*, 3719.
[42] T. F. Otero, M. Márquez, I. J. Suárez, *J. Phys. Chem. B* **2004**, *108*, 15429.
[43] A. J. Fernández Romero, J. J. López Cascales, T. Fernández Otero, *J. Phys. Chem. B* **2005**, *109*, 907.
[44] J. J. López Cascales, A. J. Fernández, T. F. Otero, *J. Phys. Chem. B* **2003**, *107*, 9339.
[45] J. J. López Cascales, T. F. Otero, *J. Chem. Phys.* **2004**, *120*, 1951.
[46] I. J. Suárez, T. F. Otero, M. Márquez, *J. Phys. Chem. B* **2005**, *109*, 1723.
[47] T. F. Otero, I. Boyano, *Electrochim. Acta* **2006**, *51*, 6238.
[48] B. J. West, T. F. Otero, B. Shapiro, E. Smela, *J. Phys. Chem. B* **2009**, *113*, 1277.
[49] T. F. Otero, J. G. Martinez, *J. Solid State Electron.* **2011**, *15*, 1169.
[50] Q. Pei, O. Inganäs, *J. Phys. Chem.* **1993**, *97*, 6034.
[51] Q. Pei, O. Inganäs, *J. Phys. Chem.* **1992**, *96*, 10507.
[52] J. Heinze, M. Stoerzbach, J. Mortensen, *Ber. Bunsen Phys. Chem.* **1987**, *91*, 960.
[53] S. Sunde, G. Hagen, R. Odegard, *J. Electrochem. Soc.* **1991**, *138*, 2561.
[54] T. Sata, *J. Membrane Sci.* **1992**, *72*, 43.
[55] P. Audebert, P. Aldebert, N. Girault, T. Kaneko, *Synth. Met.* **1993**, *53*, 251.
[56] Y. M. Volfkovich, V. S. Bagotzky, T. K. Zolotova, E. Y. Pisarevskaya, *Electrochim. Acta.* **1996**, *41*, 1905.
[57] G. Zotti, S. Zecchin, *Synth. Met.* **1997**, *87*, 115.
[58] M. F. Suárez, R. G. Compton, *J. Electroanal. Chem.* **1999**, *462*, 211.
[59] M. Bahrami-Samani, C. D. Cook, J. D. Madden, G. M. Spinks, P. G. Whitten, *Thin Solid Films.* **2008**, *516*, 2800.
[60] B. Guo, A. Finne-Wistrand, A.-C. Albertsson, *Chem. Mater.* **2011**, *23*, 1254.
[61] T. F. Otero, J. M. García de Otazo, *Synth. Met.* **2009**, *159*, 681.
[62] J. Roncali, L. H. Shi, F. Garnier, *J. Phys. Chem.* **1991**, *95*, 8983.
[63] L. Bay, T. Jacobsen, S. Skaarup, K. West, *J. Phys. Chem. B.* **2001**, *105*, 8492.
[64] A. G. Bedekar, S. F. Patil, R. C. Patil, K. Vijayamohanan, *Mater. Chem. Phys.* **1997**, *48*, 76.
[65] M. Grzeszczuk, P. Poks, *Synth. Met.* **1998**, *98*, 25.
[66] E. V. Ovsyannikova, O. N. Efimov, A. P. Moravsky, R. O. Loutfy, E. P. Krinichnaya, N. M. Alpatova, *Russ. J. Electrochem.* **2005**, *41*, 439.
[67] S.-F. Hong, S.-C. Hwang, L.-C. Chen, *Electrochim. Acta* **2008**, *53*, 6215.
[68] G. Xu, W. Wang, X. Qu, Y. Yin, L. Chu, B. He, H. Wu, J. Fang, Y. Bao, L. Liang, *Eur. Polym. J.* **2009**, *45*, 2701.
[69] K. Aoki, J. Cao, Y. Hoshino, *Electrochim. Acta* **1993**, *38*, 1711.
[70] A. F. Diaz, J. A. Logan, *J. Electroanal. Chem.* **1980**, *111*, 111.
[71] J. B. Schlenoff, H. Xu, *J. Electrochem. Soc.* **1992**, *139*, 2397.
[72] T. F. Otero, M. J. Ariza, *J. Phys. Chem. B* **2003**, *107*, 13954.
[73] L. Valero, J. Arias-Pardilla, M. Smit, J. Cauich-Rodríguez, T. F. Otero, *Polym. Int.* **2010**, *59*, 337.
[74] D.-S. Park, Y.-B. Shim, S.-M. Park, *J. Electrochem. Soc.* **1993**, *140*, 2749.
[75] H.-P. Welzel, G. Kossmehl, H.-J. Stein, J. Schneider, W. Plieth, *Electrochim. Acta* **1995**, *40*, 577.
[76] Y. Kunugi, Y. Harima, K. Yamashita, J. Ohshita, A. Kunai, M. Ishikawa, *J. Electroanal. Chem.* **1996**, *414*, 135.
[77] P. A. Christensen, A. Hamnett, *Electrochim. Acta* **1991**, *36*, 1263.
[78] P. Schottland, K. Zong, C. L. Gaupp, B. C. Thompson, C. A. Thomas, I. Giurgiu, R. Hickman, K. A. Abboud, J. R. Reynolds, *Macromolecules* **2000**, *33*, 7051.
[79] U. Barsch, F. Beck, *Electrochim. Acta* **1996**, *41*, 1761.
[80] B. Krische, M. Zagorska, *Synth. Met.* **1989**, *28*, 257.
[81] Z. Gao, Z. Minxian, C. Beshen, *J. Electroanal. Chem.* **1994**, *373*, 141.
[82] S. Ghosh, G. A. Bowmaker, R. P. Cooney, J. M. Seakins, *Synth. Met.* **1998**, *95*, 63.
[83] I. Rodríguez, B. R. Scharifker, J. Mostany, *J. Electroanal. Chem.* **2000**, *491*, 117.
[84] J. C. Thiéblemont, J. L. Gabelle, M. F. Planche, *Synth. Met.* **1994**, *66*, 243.
[85] C. Masalles, J. Llop, C. Viñas, F. Teixidor, *Adv. Mater.* **2002**, *14*, 826.
[86] A. S. Saraç, G. Sönmez, F. Ç. Cebeci, *J. Appl. Electrochem.* **2003**, *33*, 295.
[87] Z. Qi, P. G. Pickup, *Anal. Chem.* **1993**, *65*, 696.